Int J Clin Exp Pathol 2017;10(4):4047-4057
www.ijcep.com /ISSN:1936-2625/IJCEP0036863

Original Article

Mir-367 is downregulated in coronary artery disease and its overexpression exerts anti-inflammatory effect via inhibition of the NF-κB-activated inflammatory pathway

Jingzhi Sun, Caiyun Shen, Xin Jin, Xia Li, Deguang Wu

Affiliated Hospital of Jining Medical University, Jining, Shandong, China

Received July 15, 2016; Accepted September 29, 2016; Epub April 1, 2017; Published April 15, 2017

Abstract: In this study, we aimed to scrutinize the link between the expression of circulating mir-367 and the NF-κB activated inflammatory pathway in the pathogenesis of coronary artery disease (CAD) and the potential underlying molecular mechanism. Plasma samples were collected from a single cohort of 60 CAD patients and 60 control subjects, and mir-367 levels in samples stemming from each study subject were examined by quantitative real-time PCR (qRT-PCR). Simultaneously, plasma TNF-α, IL-6 and NF-κB levels were measured by ELISA. Western blotting and qRT-PCR were equally applied to determine the expression of a set of proteins. The results showed that the expression level of mir-367 was decreased in the plasma of CAD patients compared with healthy controls while levels of NF-κB, IL-6 and TNF-α increased considerably. Kendall, Spearman and Pearson correlation analyses indicated that decreased mir-367 levels were significantly correlated with elevated levels of NF-κB, IL-6 and TNF-α. Receiver-operator curve (ROC) analysis showed the potential of mir-367 as a non-invasive biomarker for CAD diagnosis with an area under-curve (AUC) of 0.9697. Furthermore, *in vitro* studies showed that silencing of mir-367 in human aortic endothelial cells (HAECs) treated with oxLDL promoted the expression of NF-κB mediated inflammatory pathways while mir-367 mimic downregulated these pathways. Further analysis pointed to a role of mir-367 in the inhibition of NF-κB inflammatory pathways via negative regulation of EFR3A and upregulation of FBXW7, probably through the Akt/mTOR pathway. Conclusively, circulating mir-367 may be a new biomarker, a potential diagnostic tool and a candidate therapeutic target for CAD.

Keywords: Coronary artery disease (CAD), mir-367, inflammation, biomarkers

Introduction

Coronary artery disease (CAD), a sequel of atherosclerosis, a local chronic inflammatory disease of arteries, is the foremost cause of morbidity and mortality in the elderly (≥ 65 years of age) patients with cardiovascular disease worldwide [1]. Despite recent advances in the diagnosis of CAD, the development of novel diagnostic noninvasive biomarkers is vital for strengthening therapeutic interventions and reducing CAD incidence [2]. Due to false positive measurements in protein-based biomarkers and because of the impossibility to discriminate non-coronary chest pain (NCCP) from troponin-negative unstable angina pectoris (UAP), circulating miRNAs are being considered as highly sensitive noninvasive disease-specific candidate biomarkers for early diagnosis of CAD [3, 4].

MicroRNAs are short noncoding RNAs (~18-22 nucleotides long) regulating post-transcription or translation of target genes by attaching to their 3'-untranslated region (3'-UTR). Up to date, a large set of microRNAs have been identified and incriminated in cardiovascular diseases as well as progression of CAD [5-11]. One of the characteristic processes preceding initiation and progression of atherosclerosis is a chronic vascular inflammation which is instigated by the release of pro-inflammatory cytokines via activation of Nuclear factor-κB (NF-κB) pathway [12]. A previous study revealed that TNF-indu-

ced microRNAs control the expression of inflammation in endothelial cells [13]. MicroRNA-10a, microRNA-181b, microRNA-146 and microRNA-126 have been equally reported as inflammation mediators in endothelium cells located within athero-susceptible regions [14-17]. A large review [18] on the regulation of atherosclerosis by microRNAs has been recently published and provided comprehensible data on the role and mechanisms of a variety of these microRNAs.

In a recent microarray study of peripheral blood mononuclear cells (PBMCs), it has been demonstrated that miR-367, as well as other microRNAs were undetected in PBMCs from both control and CAD patients [19]. However, expression profiling based on DNA microarray for patients experiencing off-pump coronary artery bypass surgery revealed that mir-367 was involved in gene regulation of ERG2 [19]. Furthermore, a recent study demonstrated that miR-367 represses IRAK4 and, thus, plays a fundamental role in the regulation of inflammation in intracerebral hemorrhage, suggesting that mir-367 may constitute a critical biomarker in inflammatory diseases such as CAD [20]. In addition, despite its potential as a diagnostic biomarker of a variety of diseases such cancers [21-24], much accurate assessment of the expression pattern, the functional role and the possible regulatory mechanism instigated by circulating miR-367 in CAD has not been performed.

Therefore, in this study, we aimed to evaluate the plasma levels of miR-367 in CAD patients in order to uncover its potentiality as novel noninvasive biomarkers for diagnosis of CAD and explore its possible role on the regulation of NF-κB induced inflammatory pathways and the underlying mechanisms.

Materials and methods

Study population

This study was performed in conformity with the principles of the Declaration of Helsinki and was approved by the Medical Ethics Committee of the Affiliated Hospital of Jining Medical University, Shandong, China. Written informed consent was obtained from each subject or his legal representative before enrollment. A total of sixty diagnostically confirmed CAD patients and sixty healthy individuals were enrolled in this study at the Affiliated Hospital of Jining Medical University. CAD diagnostic was determined by quantitative coronary angiography and only subjects presenting at least one major epicardial vessel with ≥ 50% stenosis as assessed by two independent experts who visually estimated luminal narrowing in multiple segments according to the AHA/ACC classification of the coronary tree were considered as suffering from CAD. All the participants included in the study were age of 62 to 79 years. Individuals exhibiting at least one of the symptoms including elevated creatine kinase (CK-MB) or cardiac troponin I (cTnI) levels, decreased left ventricular ejection fraction (LVEF) ≤ 45%, acute myocardial infarction (AMI), congestive heart failure, severe renal and hepatic dysfunction and ongoing inflammatory and malignant disease were excluded from the study. All the controls had no history of CAD or stroke with reports of ECG, ETT and echocardiogram in the regular range, were not diagnosed for any hepatic or renal disease and were not hospitalized for at least 6 weeks before the beginning of the study.

Plasma samples collection

Samples (5 mL) of peripheral blood were collected from patients and healthy subjects in EDTA coated tubes and treated within 1 hour. Following collection, plasma was separated from blood and samples centrifuged for 15 min (4°C 1,500× g). After a second centrifugation of the supernatants in the same conditions, the obtained pure plasma was transferred to RNase-free tubes and stored at -80°C until use.

Cell culture, oxLDL treatment and transient transfection

Cryopreserved human aortic endothelial cells (HAECs) (Genlantis, San Diego, CA, USA; PH30-405AK, Lot 2248) were incubated in 50 μg/ml rat tail collagen type 1-coated (BD Biosciences, Bedford, MA, USA) culture flasks and grown in EC growth medium-2 (Lonza, Allendale, NJ, USA), supplemented with 1% antibiotic-antimycotic solution (Invitrogen) and 10% fetal bovine serum (Thermo Scientific-Hyclone, Waltham, MA, USA; CC-3162). Subsequently, HAECs were cultured to 75-90% confluence and fourth passage HAECs used for experiments.

Table 1. Primers used in this study

Gene	Sense primer	Antisense primer
hsa-mir-367	5'-GTGGTTCCTACCTAATCAGC 3'	5'-GGAAAAGGATACTGGAGATC 3'
DNAJB9	5'-ATGGCTACTCCCCAGTCAATTTTCA 3'	5'-TGAAAATTGACTGGGGAGTAGCCAT 3'
SYNJ1	5'-ATGCGGAAGAGATGGGCCTGCTGGA 3'	5'-TCCAGCAGGCCCATCTCTTCCGCAT 3'
HIPK3	5'-ATGGCCTCACAAGTCTTGGTCTACC 3'	5'-GGTAGACCAAGACTTGTGAGGCCAT 3'
FBXW7	5'-CCACTGGGCTTGTACCATGTT-3'	5'-CAGATGTAATTCGGCGTCGTT-3'
CD69	5'-ATGAGCTCTGAAAATTGTTTCGTAG 3'	5'-CTACGAAACAATTTTCAGAGCTCAT 3'
EFR3A	5'-ATGCCTACCCGAGTATGCTGCTGCT 3'	5'-AGCAGCAGCATACTCGGGTAGGCAT 3'

HAECs were randomly divided into six groups: a normal control group, an oxLDL group and groups of oxLDL-induced HAECs transfected with mir-367 mimic (MISSION® microRNA Mimic hsa-miR-367, Sigma Aldrich) and anti-mir-367 (miRZip-367 anti-miR-367 microRNA construct, System Biosciences). Cells in the control group were incubated under the normal growth conditions. The HAECs in the oxLDL group were incubated for 24 hours with medium containing 200 μg/mL oxLDL. The oxLDL was prepared from normal plasma samples as previously described [25]. In the mimic or anti-mir groups, the cells were transfected with mir- or anti-mir-367 using Lipofectamine transfection system. For expression analyses, HAECs were stimulated with TNF-α and/or IL-6 at a concentration of 0.3 ng/ml. To determine the functional role of FBXW7 and EFR3A, FBXW7 siRNA (Thermo Fisher Scientific) and EFR3A siRNA (Thermo Fisher Scientific) were individually transfected or co-transfected into above cell groups according to the manufacturer's guidelines.

Enzyme-linked immunosorbent assay (ELISA) of inflammatory markers

Cell or plasma supernatants were analyzed to determine the concentrations of NF-κB, TNF-α and IL-6 using human ELISA kits (Thermo Fisher Scientific) following the manufacturer's guidelines.

Mir-367 target gene prediction

Mir-367 target genes were predicted using the online bioinformatics tool miRDB (http://www.mirdb.org/miRDB/).

RNA extraction and RT-PCR

Total RNA was isolated from plasma samples and HAECs using the conventional TRIzol or a TRIzol-based miRNA isolation protocol (Invitrogen) according to the manufacturer protocol, purified and quantitatively assessed for the RNA concentrations using NanoDrop ND-1000 spectrophotometer (NanoDrop Technologies Inc., Wilmington, USA) and kept at -80°C until use. Real-time quantitative reverse-transcription PCR (qRT-PCR) was employed for measuring the expression of mir-367, DNAJB9, SYNJ1, HIPK3, FBXW7, CD69 and EFR3A. Around 4 μL of extracted total RNA was reverse-transcribed into cDNA at 42°C for 30 minutes using ABM miRNA EasyScript cDNA Synthesis kit (Cat No. G269) following the vendors' instructions. The qRT-PCR experiment was achieved with the QuantiFast SYBR Green PCR Kit (Qiagen, Germany) according to the manufacturer's protocol using a reaction volume of 20 μl. The PCR cycling condition was set as follows: 95°C for 5 min, 40 cycles of 95°C for 15 s, 60°C for 15 s and 72°C for 20 s. The fluorescence intensity was determined by the Bio-Rad CFX96™ Real-Time System. The relative level of mRNA for each gene was normalized to that of GAPDH and miR-156a was used as the normalization control for mir-367. The sequences of the primers used are listed in **Table 1**. The relative expression of a specific RNA was calculated by the comparative Ct method.

Western blot analyses

Plasma or HAECs were lysed in a modified RIPA buffer (150 mM NaCl, 10 mM Tris, pH 7.4, 1 mM EDTA, 1% Triton X-100, 1% deoxycholic acid, 1 mM PMSF, with addition of complete TM protease inhibitor cocktail). Protein concentrations were quantified using a BCA assay. After purification by SDS-PAGE, aliquots were transferred to a PVDF membrane (Millipore, USA). The membrane was blocked at RT for 2 h in 5% nonfat dry milk diluted with TBST (in mM: Tris-

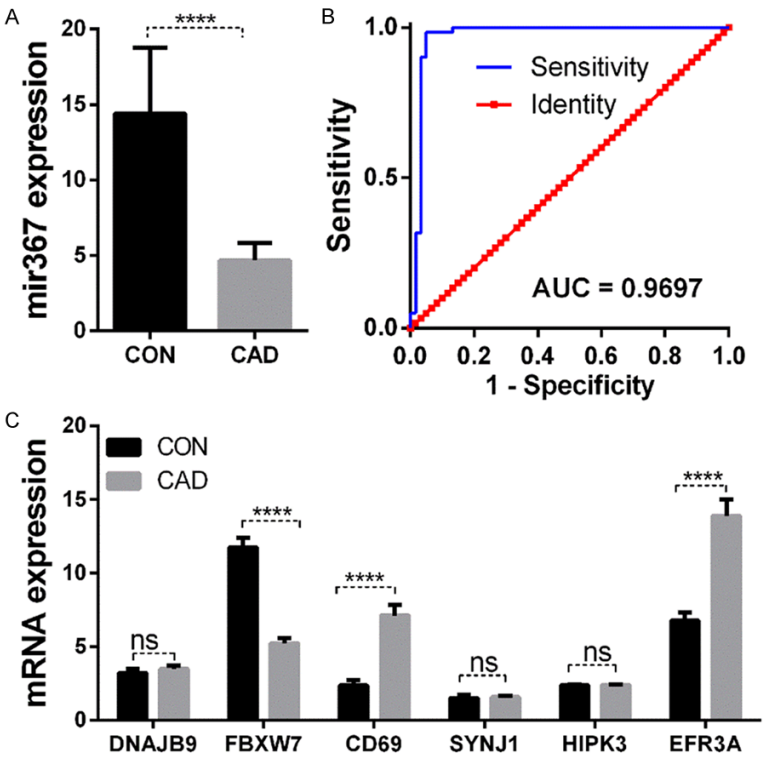

Figure 1. Relative expression levels of mir-367 and its targets in plasma from CAD patients and healthy individuals and diagnostic value of mir-367. A: Expression of mir-367 in plasma from CAD patients (n = 60) and healthy controls (n = 60). Total RNA was isolated from plasma sample stemming from each individual, reverse-transcribed, and subjected to real-time PCR analysis. B: ROC curve of mir-367 expression in CAD patients and healthy individuals. C: Expression of predicted mir-367 targets in plasma of CAD patients and healthy individuals. Data are represented as mean ± SEM; ****; P < 0.0001 in intergroup comparisons, ns; non-significant.

HCl 20, NaCl 150, pH 7.5, 0.1% Tween 20). The membrane was incubated overnight at 4°C with a polyclonal mouse anti-human GAPDH, FBXW7, EFR3A, Akt, p-Akt, mTOR, p-mTOR, IKKα, IKKβ, IKKγ, NF-κB and IκB (1:500 dilution; ABCAM, Shanghai, CHINA). After washing in TBS-T, the membrane was incubated for 1 h with a goat anti-rabbit IgG conjugated to horseradish peroxidase (1:10000 dilution; Santa Cruz Biotechnology Inc. USA). At last, the protein levels were determined using Amersham ECLTM western blotting detection reagents (GE Healthcare, UK). GAPDH was employed as the loading sample control. Relative intensities of protein bands were analyzed by Scan-gel-it software.

Statistical analysis

Graphs were constructed using GraphPad Prism version 6 for Windows (GraphPad Software, San Diego, CA, USA) and reported as mean ± SEM/SD. For comparison of variables among groups, Student's *t*-test, One-way ANOVA or two-way ANOVA followed by Bonferroni posttests were used as appropriate. The correlations between parameters were measured with Pearson, Kendall and Spearman correlation analyses. The receiver operating characteristic (ROC) curves were used for discriminating CAD patients from the healthy subjects. P < 0.05 was considered statistically significant.

Results

Expression of circulating mir-367 and mir-367 targets in CAD and its diagnostic value

To investigate the characteristics of mir-367 as plasma potential biomarkers of CAD, RT-PCR analysis was performed to detect the mRNA level of mir-367. The results (**Figure 1A**) showed that mir-367 was significantly (P = 0.0001) decreased in the CAD group (4.670 ± 0.1528 relative expression, n = 60) compared with the control group (14.43 ± 0.5615 relative expression, n = 60). To investigate the diagnostic accuracy of circulatory mir-367 as potential biomarkers of CAD, ROC curve analysis was performed. The ROC curve of mir-367 (**Figure 1B**) reflected a significant separation between CAD patients and controls with an area under curve (AUC) of 0.9697 for the diagnosis of CAD patients. It was suggested that circulating mir-367 might be used as a potential biomarker for early diagnosis of CAD patients.

To clarify the potential mechanism of mir-367 in the regulation of the CAD inflammatory response, the putative targets of mir-367 were first identified using the bioinformatics tool miRDB. The results showed that there were 495 predicted targets for mir-367 in miRDB

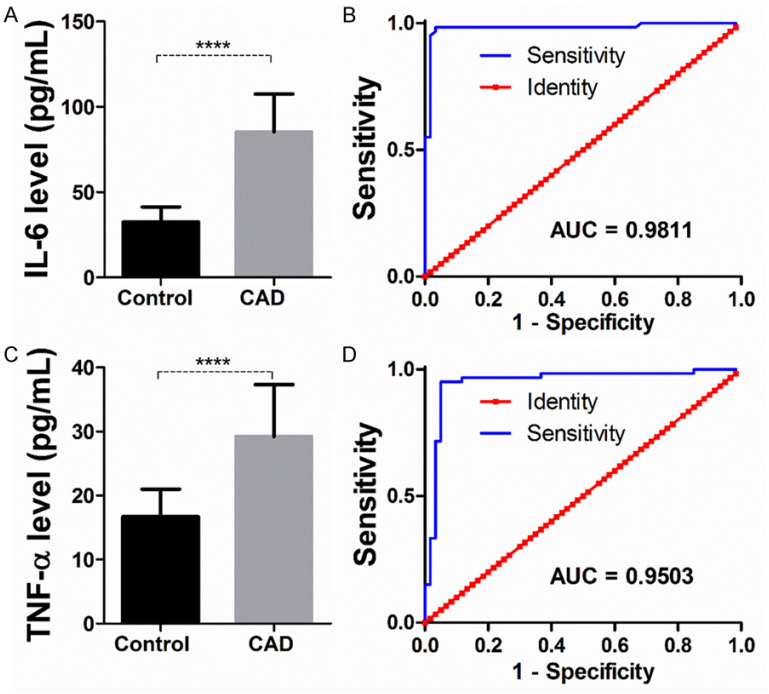

Figure 2. Changes in levels of inflammatory cytokines IL-6 and TNF-α in plasma of CAD patients vs. healthy individuals. A: Levels of IL-6 in CAD (n = 60) and control individuals (n = 60). B: ROC curve of IL-6 levels in CAD and control individuals. C: Levels of TNF-α in CAD (n = 60) and control individuals (n = 60). D: ROC curve of TNF-α levels in CAD and control individuals. IL-6 = interleukin-6; TNF-α = tumor necrosis factor alpha. Data are expressed as means ± SEM; ****; P < 0.0001 in intragroup comparisons.

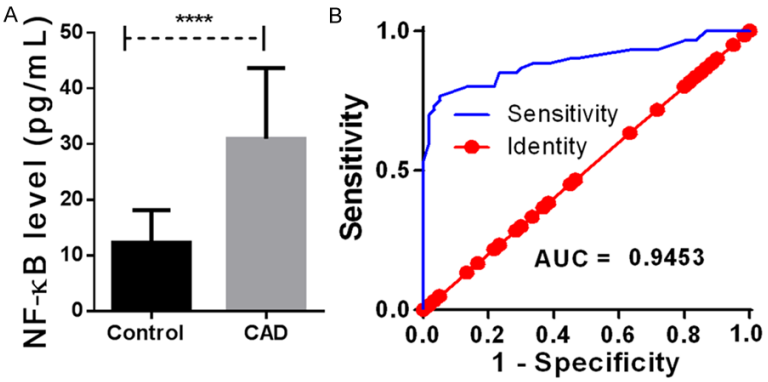

Figure 3. NF-κB levels in CAD patients and control individuals and potential diagnostic value. A: NF-κB concentration was measured in CAD patients (n = 60) and control individuals (n = 60) using ELISA test. B: ROC curve of NF-κB levels in CAD patients and control individuals. Values are expressed as means ± SEM (n = 60). ****; P < 0.0001 in intragroup comparisons.

(data not shown). Of these predicted targets, the mRNA expression of 6 presenting 100% target score was explored. The results (**Figure 1C**) showed that FBXW7 was significantly down-regulated while the expressions of CD69 and EFR3A were significantly up-regulated in the CAD patients compared with the control group. No significant changes were observed concerning the mRNA levels of DNAJB9, SYNJ1 and HIPK3. These results suggested that mir-367 may be implicated in CAD pathogenesis by targeting FBXW7, CD69 and/or EFR3A.

Levels of inflammation markers and NF-κB activation in plasma of CAD patients

To evaluate the contribution of mir-367 in CAD inflammation, we measured the levels of inflammatory markers including IL-6, TNF-α and NF-κB. As shown in **Figure 2A** and **2C**, CAD patients had significantly (P < 0.0001) higher plasma levels of circulating IL-6 (85.30 ± 2.851 pg/ml, n = 60 for CAD group and 32.43 ± 1.155 pg/ml, n = 60 for control group) and TNF-α (29.23 ± 1.044 pg/ml, n = 60 for CAD group and 16.68 ± 0.5578 pg/ml, n = 60 for control group). The ROC curve of IL-6 and TNF-α (**Figure 2B**, **2D**) showed strong coincidences of high levels of these cytokines with CAD patients with an area under curve (AUC) of 0.9811 and 0.9503, respectively.

The measurement of NF-κB levels using ELISA test revealed (**Figure 3A**) significantly increased release of NF-κB in CAD patients (43.40 ± 2.366, n = 60) compared to control individuals (12.28 ± 0.7548, n = 60). The ROC curve of NF-κB (**Figure 3B**) showed a strong association of high levels of NF-κB with CAD (AUC = 0.9453), which implied the functional inflammatory role of NF-κB in CAD. Real-time PCR (RT-PCR) (**Figure 4A**) and western blot (**Figure 4B**, **4C**) analyses

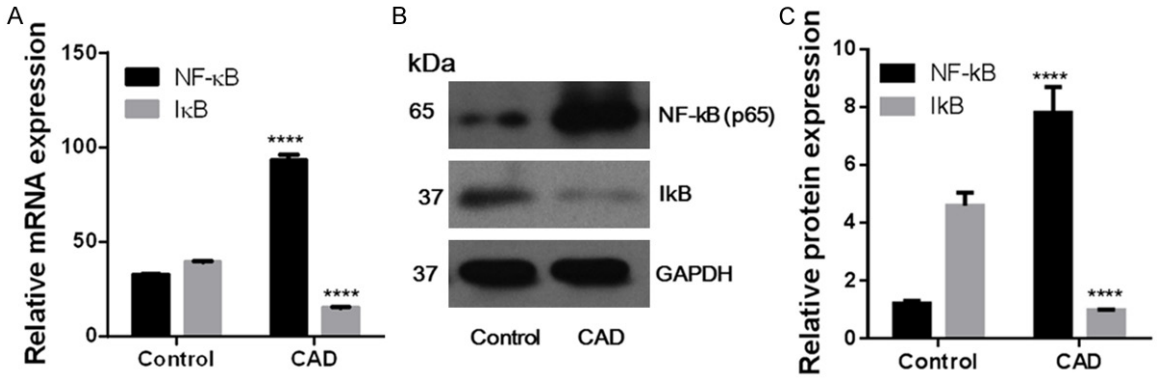

Figure 4. mRNA and protein expression of NF-κB and IκB in CAD patients and control individuals. A: The quantitative fold changes in mRNA expression were determined as relative to GAPDH mRNA levels in each corresponding group and calculated using the $2^{-\Delta\Delta CT}$ method. B, C: Western blot analysis and densitometrical quantitation of NF-κB and IκB expression in each group. Values are expressed as means ± SD. ****; P < 0.0001 vs. control.

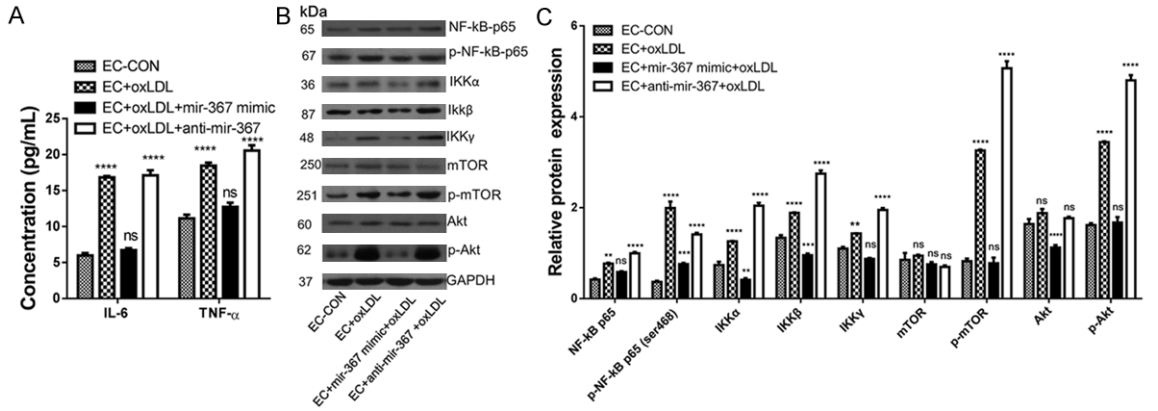

Figure 5. Overexpression of mir-367 inhibits the NF-κB signaling pathway in oxLDL-induced HAECs. (A) mir-367 decreases the levels of IL-6 and TNF-α in oxLDL-induced HAECs. (B, C) Western blotting analysis (B) and densitometrical quantitation (C) of blots obtained from the expression analysis of proteins in the NF-κB signaling, mTOR, p-mTOR, Akt and p-Akt in different groups of oxLDL-induced HAECs. ****; P < 0.0001 vs. control, ***; P < 0.001 vs. control, **; P < 0.01 vs. control, ns; non-significant.

equally showed a significant (P < 0.0001) increase in the expression of NF-κB in CAD patients comparatively to the control group. Conversely, the measurement of IκB expression showcased inverse trends with a significant difference between both groups (54.8 ± 2.8 and 15.1 ± 0.35, for control and CAD patients, respectively, P < 0.0001).

Correlation of mir-367 with inflammatory markers

To evaluate the interference of mir-367 with inflammation in CAD, we equally performed Kendall, Spearman and Pearson correlation analyses and found that plasma levels of miR-367 were significantly correlated with plasma levels of TNF-α, IL-6 and NF-κB in CAD patients (Table S1). This suggested the functional role of mir-367 in the pathophysiology of CAD, especially in the regulation of inflammation pathways.

Overexpression of mir-367 inhibits the NF-κB signaling pathway in oxLDL-induced human aortic endothelial cells in vitro

In order to elucidate the potential mechanism of inflammation mediation by mir-367, human aortic endothelial cells (HAECs) were induced by oxLDL. The results (**Figure 5A**) showed that, oxLDL treatment led to activation of IL-6 and TNF-α compared to the control group (non-treated HAECs). Similar results were obtained

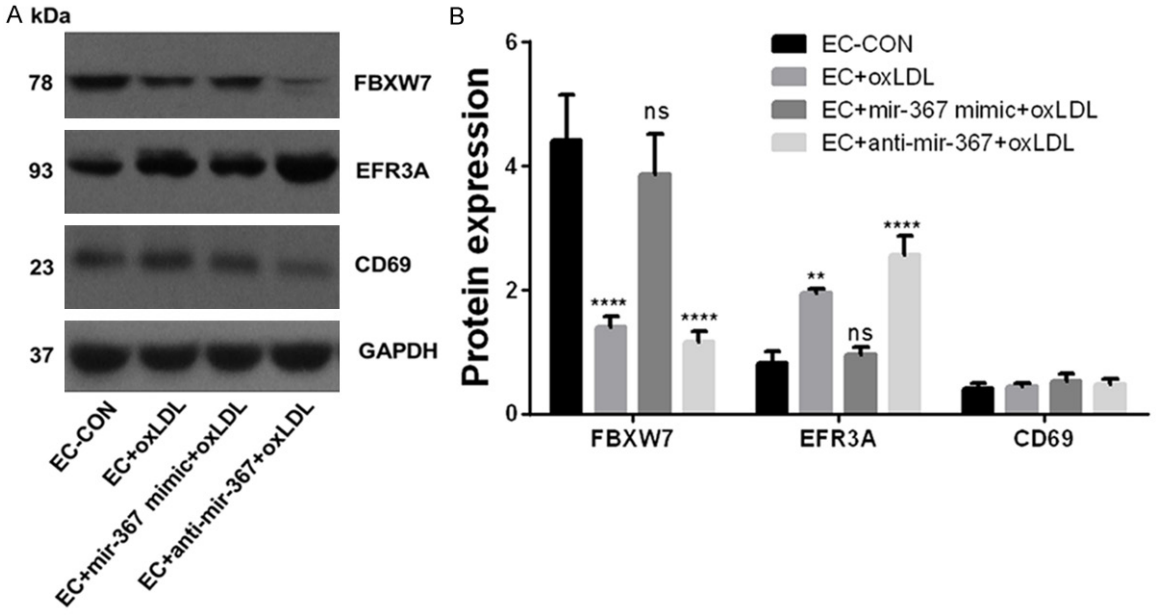

Figure 6. Effect of mir-367 overexpression on its targets in oxLDL-induced HAECs. (A) Western blotting analysis and (B) densitometric quantitation of blots obtained from the expression analysis of proteins FBXW7, EFR3A and CD69 in different groups of oxLDL-induced HAECs. mir-367 overexpression upregulated the levels of FBXW7 and downregulated EFR3A in oxLDL-induced HAECs but did not affect the expression of CD69. ****; $P < 0.0001$ vs. control, **; $P < 0.01$ vs. control and ns; non-significant.

from HAECs transfected with anti-mir-367. On the contrary, transfection of HAECs with mir-367 mimic reduced the levels of these cytokines. The above results further confirmed that mir-367 may play a fundamental role in the pathogenesis of cardiovascular diseases.

To explore the potential implication of mir-367 in the coronary inflammation, the effect of mir-367 mimic and anti-mir-367 on the expression of NF-κB and genes involved in related inflammatory pathways in oxLDL-induced endothelial cells was determined using western blotting. As shown in **Figure 5B** and **5C**, treatment with oxLDL and anti-mir-367 led to increased expression of NF-κB, IKKα, IKKβ and IKKγ, suggesting that downregulation of mir-367 induces NF-κB activation of inflammatory pathways. Similarly, significantly increased expression of phosphorylated mTOR (p-mTOR) and Akt (p-Akt) was observed in the same conditions. On the contrary, mir-367 mimic decreased the expression of above pathways and there was no significant difference comparatively to the control group. The above findings suggested that overexpression of mir-367 may inhibit the NF-κB signaling-induced inflammation by modulating the Akt/mTOR axis.

In order to get insight on the mechanism by which mir-367 operates, we also measured the expression of mir-367 targets that showed significant changes between the CAD patients and healthy controls as described above. The results (**Figure 6**) showed that mir-367 mimic led to increased expression of FBXW7 in oxLDL-induced endothelial cells while the contrary was found in oxLDL and anti-mir-367 cells. The opposite trends were observed for EFR3A whereas mir-367 or anti-mir367 did not affect CD69 expression. These results indicated that mir-367 inhibits the NF-κB-activated inflammatory pathway by targeting FBXW7 and EFR3A. To confirm FBXW7 and EFR3A as mir-367 targets in the regulation of inflammatory pathways in CAD, FBXW7 siRNA and/or EFR3A siRNA were transfected in TNF-α and/or IL-6 treated HAECs and the expression of NF-κB measured. The results (**Figure 7A**) indicated that in TNF-α + IL-6-treated cells, the simultaneous transfection of FBXW7 siRNA and EFR3A siRNA led to increased expression of NF-κB. In the same cell type, the EFR3A siRNA led to significantly higher and increased NF-κB expression while FBXW7 siRNA did not significantly affect this expression. In TNF-α-treated HAECs, the expression of NF-κB was increased by FBXW7 siRNA

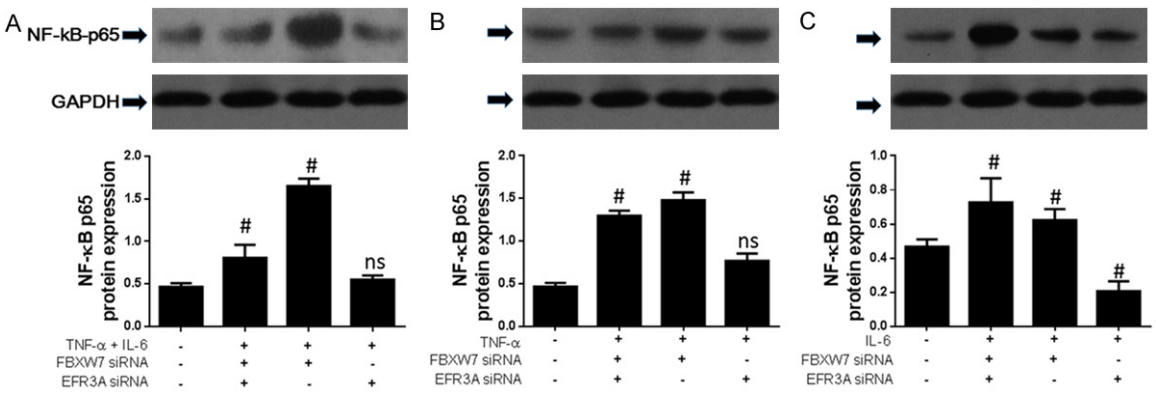

Figure 7. Silencing of mir-367 targets decreases the activation of NF-κB in IL6-, TNF-α- or IL-6 + TNF-α-induced HAECs expressing mir-367. Western blotting analysis and densitometrical quantitation of blots obtained from the expression analysis of NF-κB and IκB in IL-6 + TNF-α- (A), TNF-α- (B) or IL6- (C) induced HAECs. Upregulation of FBXW7 and downregulation of EFR3A by mir-367 inhibited the NF-κB inflammatory pathways mediated by IL-6 and TNF-α. #; $P < 0.0001$ vs. control, ns; non-significant.

transfection while no significant increase was recorded for EFR3A siRNA. Interestingly, in IL-6-treated HAECs, the expression of NF-κB was significantly increased by FBXW7 siRNA or transfection with both FBXW7 siRNA and EFR3A siRNA while a significantly decreased NF-κB expression was observed for EFR3A siRNA. Altogether, these findings suggested that mir-367 inhibits NF-κB-activated inflammatory pathways by negatively regulating EFR3A and upregulating FBXW7. Moreover, EFR3A may be a key mediator in IL-6/NF-κB pathway while FBXW7 may be involved in both IL-6/NF-κB and TNF-α/NF-κB pathways.

Discussion

CAD, the leading cause of death in developed countries, is the most frequent form of cardiovascular disease and comprises a broad spectrum of clinical entities with devastating outcomes such as high morbidity and mortality [26]. Though sophisticated tools have been developed for CAD diagnosis [27, 28], the pathogenesis of this disease is not well understood. This has motivated the quest for transcriptomics and proteomics-based biomarkers for differential diagnosis and to predict outcome for CAD [29, 30]. In recent years, the potential of microRNAs as biomarkers for cardiovascular diseases including CAD, have been widely reported [31-33]. The present study investigated the plasma levels of circulating miR-367 to establish its prospective role as CAD biomarkers. Our results showed that plasma levels of miR-367 were significantly ($P < 0.0001$) decreased in CAD patients comparatively to healthy controls. To the best of our knowledge, this is the first report of downregulation of mir-367 in the pathogenesis of CAD. Nevertheless, several lines of evidence suggest that mir-367 is involved in the pathogenesis of different type of cancers and in the regulation of diverse biological processes such as inflammation, cell proliferation, invasion and metastasis [19-24, 34-41]. Herein, ROC curve analysis (AUC = 0.9697) showed that mir-367 could be used as a potential diagnostic non-invasive biomarker for discriminating CAD from healthy individuals. However, our study presents limitations in the fact that it is a single-center study involving a small sample size and the specificity relatively to other cardiovascular diseases was not investigated. Therefore the present findings should be interpreted with caution.

One of the most pathological processes implicated in CAD is endothelial inflammation leading to endothelial dysfunction [42, 43]. In this study, in order to elucidate whether mir-367 is involved in the mediation of inflammation in CAD, we first measured the plasma levels of inflammation markers. Compared to non-CAD subjects, the results showed elevated levels of IL-6, TNF-α and NF-κB in CAD patients, which was indicative of the occurrence of inflammation in CAD. The ROC curve analysis also showed the potential of these markers in the diagnosis of CAD, but this observation could

lead to misinterpretation because of the incidence of inflammation in the pathophysiology of various diseases. Nevertheless, the present results were in corroboration with previous studies showing the occurrence of inflammation in CAD and other cardiovascular diseases [44-46].

Our findings equally showed that plasma levels of miR-367 were significantly correlated with plasma levels of TNF-α, IL-6 and NF-κB in CAD patients, which suggests the functional role of mir-367 in the pathophysiology of CAD. This was in conformity with previous findings stipulating that mir-367 negatively regulates inflammation in microglia [20]. To further determine the possible mechanism of mir-367 in the regulation of endothelial inflammation, *in vitro* studies were performed. The results showed that oxLDL and anti-mir-367 increases NF-κB, TNF-α and IL-6 levels as well as those of p-mTOR and p-Akt in the HAECs. On the contrary, mir-367 mimic downregulated these pathways. In addition, silencing of mir-367 targets FBXW7 and EFR3A in response to TNF-α and/or IL-6 treatment of HAECs suggested that mir-367 inhibits NF-κB-activated inflammatory pathways by negatively regulating EFR3A and upregulating FBXW7, probably through the Akt/mTOR pathway, with EFR3A as a candidate key mediator in IL-6/NF-κB axis while FBXW7 may be involved in both IL-6/NF-κB and TNF-α/NF-κB pathways.

Conclusion

Altogether, we have demonstrated that plasma levels of mir-367 are significantly decreased in CAD patients compared with healthy control individuals. Moreover, we showed that overexpression of mir-367 could inhibit NF-κB-mediated inflammatory pathways in CAD in particular, and other cardiovascular diseases in general. These results may impart useful clinical implications in the diagnosis and treatment of CAD.

Acknowledgements

This study was supported by the corresponding author's personal funds. We greatly acknowledge the generous support from the members of the study community, without which the project would not have been possible. We thank the Affiliated Hospital of Jining Medical University, which support us the platform to finish this study.

Disclosure of conflict of interest

None.

Address correspondence to: Jingzhi Sun, Affiliated Hospital of Jining Medical University, 89 Guhuai Road, Shandong, China. Tel: 0086 537-2903757; Fax: 0086 537-2213030; E-mail: jingzhisun@126.com

References

[1] Skelly AC, Hashimoto R, Buckley DI, Brodt ED, Noelck N, Totten AM, Lindner JR, Fu R and McDonagh M. AHRQ Comparative Effectiveness Reviews. In: editors. Noninvasive Testing for Coronary Artery Disease. Rockville (MD): Agency for Healthcare Research and Quality (US); 2016. pp.

[2] Ali Sheikh MS, Xia K, Li F, Deng X, Salma U, Deng H, Wei Wei L, Yang TL and Peng J. Circulating miR-765 and miR-149: Potential Noninvasive Diagnostic Biomarkers for Geriatric Coronary Artery Disease Patients. Biomed Res Int 2015; 2015: 740301.

[3] Schulte C and Zeller T. microRNA-based diagnostics and therapy in cardiovascular disease-Summing up the facts. Cardiovasc Diagn Ther 2015; 5: 17-36.

[4] Wang J, Pei Y, Zhong Y, Jiang S, Shao J and Gong J. Altered Serum MicroRNAs as Novel Diagnostic Biomarkers for Atypical Coronary Artery Disease. PLoS One 2014; 9: e107012.

[5] Ahlin F, Arfvidsson J, Vargas KG, Stojkovic S, Huber K and Wojta J. MicroRNAs as circulating biomarkers in acute coronary syndromes: A review. Vascul Pharmacol 2016; 81: 15-21.

[6] De Rosa S and Indolfi C. Circulating microRNAs as Biomarkers in Cardiovascular Diseases. EXS 2015; 106: 139-149.

[7] Gareri C, De Rosa S and Indolfi C. MicroRNAs for Restenosis and Thrombosis After Vascular Injury. Circ Res 2016; 118: 1170-1184.

[8] Schulte C, Molz S, Appelbaum S, Karakas M, Ojeda F, Lau DM, Hartmann T, Lackner KJ, Westermann D, Schnabel RB, Blankenberg S and Zeller T. miRNA-197 and miRNA-223 Predict Cardiovascular Death in a Cohort of Patients with Symptomatic Coronary Artery Disease. PLoS One 2015; 10: e0145930.

[9] Wang S, He W and Wang C. MiR-23a regulate the vasculogenesis of coronary artery disease by targeting EGFR. Cardiovasc Ther 2016; 34: 199-208.

[10] Widmer RJ, Lerman LO and Lerman A. MicroRNAs: small molecule, big potential for coronary artery disease. Eur Heart J 2016; 37: 1750-2.
[11] Xu X and Li H. Integrated microRNAgene analysis of coronary artery disease based on miRNA and gene expression profiles. Mol Med Rep 2016; 13: 3063-3073.
[12] Sun X, He S, Wara AKM, Icli B, Shvartz E, Tesmenitsky Y, Belkin N, Li D, Blackwell TS, Sukhova GK, Croce K and Feinberg MW. Systemic Delivery of MicroRNA-181b Inhibits Nuclear Factor-κB Activation, Vascular Inflammation, and Atherosclerosis in Apolipoprotein E-Deficient Mice. Circ Res 2014; 114: 32-40.
[13] Suárez Y, Wang C, Manes TD and Pober JS. TNF-induced miRNAs Regulate TNF-induced expression of E-Selectin and ICAM-1 on Human Endothelial Cells: Feedback Control of Inflammation. J Immunol 2010; 184: 21-25.
[14] Sun X, Icli B, Wara AK, Belkin N, He S, Kobzik L, Hunninghake GM, Vera MP, Registry M, Blackwell TS, Baron RM and Feinberg MW. MicroRNA-181b regulates NF-κB-mediated vascular inflammation. J Clin Invest 2012; 122: 1973-1990.
[15] Cheng HS, Sivachandran N, Lau A, Boudreau E, Zhao JL, Baltimore D, Delgado-Olguin P, Cybulsky MI and Fish JE. MicroRNA-146 represses endothelial activation by inhibiting pro-inflammatory pathways. EMBO Mol Med 2013; 5: 949-966.
[16] Harris TA, Yamakuchi M, Ferlito M, Mendell JT and Lowenstein CJ. MicroRNA-126 regulates endothelial expression of vascular cell adhesion molecule 1. Proc Natl Acad Sci U S A 2008; 105: 1516-1521.
[17] Fang Y, Shi C, Manduchi E, Civelek M and Davies PF. MicroRNA-10a regulation of proinflammatory phenotype in athero-susceptible endothelium in vivo and in vitro. Proc Natl Acad Sci U S A 2010; 107: 13450-13455.
[18] Feinberg MW and Moore KJ. MicroRNA Regulation of Atherosclerosis. Circ Res 2016; 118: 703-720.
[19] Sun Y, Gao Y, Sun J, Liu X, Ma D, Ma C and Wang Y. Expression profile analysis based on DNA microarray for patients undergoing off-pump coronary artery bypass surgery. Exp Ther Med 2016; 11: 864-872.
[20] Yuan B, Shen H, Lin L, Su T, Zhong L and Yang Z. MicroRNA367 negatively regulates the inflammatory response of microglia by targeting IRAK4 in intracerebral hemorrhage. J Neuroinflammation 2015; 12: 206.
[21] Meng X, Lu P and Fan Q. miR-367 promotes proliferation and invasion of hepatocellular carcinoma cells by negatively regulating PTEN. Biochem Biophys Res Commun 2016; 470: 187-191.
[22] Sun J, Song K, Feng X and Gao S. MicroRNA-367 is a potential diagnostic biomarker for patients with esophageal squamous cell carcinoma. Biochem Biophys Res Commun 2016; 473: 363-369.
[23] Syring I, Bartels J, Holdenrieder S, Kristiansen G, Muller SC and Ellinger J. Circulating serum miRNA (miR-367-3p, miR-371a-3p, miR-372-3p and miR-373-3p) as biomarkers in patients with testicular germ cell cancer. J Urol 2015; 193: 331-337.
[24] Yang SL, Yang M, Herrlinger S, Liang C, Lai F and Chen JF. MiR-302/367 regulate neural progenitor proliferation, differentiation timing, and survival in neurulation. Dev Biol 2015; 408: 140-150.
[25] Wang YK, Hong YJ, Yao YH, Huang XM, Liu XB, Zhang CY, Zhang L and Xu XL. 6-Shogaol Protects against Oxidized LDL-Induced Endothelial Injruries by Inhibiting Oxidized LDL-Evoked LOX-1 Signaling. J Evid Based Complementary Altern Med 2013; 2013: 13.
[26] Dai X, Wiernek S, Evans JP and Runge MS. Genetics of coronary artery disease and myocardial infarction. World J Cardiol 2016; 8: 1-23.
[27] O'Rourke RA, Brundage BH, Froelicher VF, Greenland P, Grundy SM, Hachamovitch R, Pohost GM, Shaw LJ, Weintraub WS and Winters WL. American College of Cardiology/American Heart Association Expert Consensus document on electron-beam computed tomography for the diagnosis and prognosis of coronary artery disease. J Am Coll Cardiol 2000; 36: 326-340.
[28] Parker MW, Iskandar A, Limone B, Perugini A, Kim H, Jones C, Calamari B, Coleman CI and Heller GV. Diagnostic accuracy of cardiac positron emission tomography versus single photon emission computed tomography for coronary artery disease a bivariate meta-analysis. Circ Cardiovasc Imaging 2012; 5: 700-707.
[29] Satoh K, Fukumoto Y, Sugimura K, Miura Y, Aoki T, Nochioka K, Tatebe S, Miyamichi-Yamamoto S, Shimizu T and Osaki S. Plasma cyclophilin A is a novel biomarker for coronary artery disease. Circ J 2013; 77: 447-455.
[30] Ren J, Zhang J, Xu N, Han G, Geng Q, Song J, Li S, Zhao J and Chen H. Signature of circulating microRNAs as potential biomarkers in vulnerable coronary artery disease. PLoS One 2013; 8: e80738.
[31] Creemers EE, Tijsen AJ and Pinto YM. Circulating microRNAs novel biomarkers and extracellular communicators in cardiovascular disease? Circ Res 2012; 110: 483-495.
[32] Olson EN. MicroRNAs as therapeutic targets and biomarkers of cardiovascular disease. Sci Transl Med 2014; 6: 239ps3.

[33] Tijsen AJ, Pinto YM and Creemers EE. Circulating microRNAs as diagnostic biomarkers for cardiovascular diseases. Am J Physiol Heart Circ Physiol 2012; 303: H1085-H1095.
[34] Bin Z, Dedong H, Xiangjie F, Hongwei X, Qinghui Y. The microRNA-367 inhibits the invasion and metastasis of gastric cancer by directly repressing Rab23. Genet Test Mol Biomarkers 2015; 19: 69-74.
[35] Campayo M, Navarro A, Vinolas N, Diaz T, Tejero R, Gimferrer JM, Molins L, Cabanas ML, Ramirez J, Monzo M and Marrades R. Low miR-145 and high miR-367 are associated with unfavourable prognosis in resected nonsmall cell lung cancer. Eur Respir J 2013; 41: 1172-1178.
[36] Chae YS, Kim JG, Kang BW, Lee SJ, Lee YJ, Park JS, Choi GS, Lee WK and Jeon HS. Functional polymorphism in the MicroRNA-367 binding site as a prognostic factor for colonic cancer. Anticancer Res 2013; 33: 513-519.
[37] Guan Y, Chen L, Bao Y, Qiu B, Pang C, Cui R and Wang Y. High miR-196a and low miR-367 cooperatively correlate with unfavorable prognosis of high-grade glioma. Int J Clin Exp Pathol 2015; 8: 6576-6588.
[38] Jeong HS, Lee JM, Suresh B, Cho KW, Jung HS and Kim KS. Temporal and Spatial Expression Patterns of miR-302 and miR-367 During Early Embryonic Chick Development. Int J Stem Cells 2014; 7: 162-166.
[39] Kaid C, Silva PB, Cortez BA, Rodini CO, Semedo-Kuriki P and Okamoto OK. miR-367 promotes proliferation and stem-like traits in medulloblastoma cells. Cancer Sci 2015; 106: 1188-1195.
[40] Zhang L, Liu Y, Song F, Zheng H, Hu L, Lu H, Liu P, Hao X, Zhang W and Chen K. Functional SNP in the microRNA-367 binding site in the 3'UTR of the calcium channel ryanodine receptor gene 3 (RYR3) affects breast cancer risk and calcification. Proc Natl Acad Sci U S A 2011; 108: 13653-13658.
[41] Zhu Z, Xu Y, Zhao J, Liu Q, Feng W, Fan J and Wang P. miR-367 promotes epithelial-to-mesenchymal transition and invasion of pancreatic ductal adenocarcinoma cells by targeting the Smad7-TGF-beta signalling pathway. Br J Cancer 2015; 112: 1367-1375.
[42] Hansson GK. Inflammation, atherosclerosis, and coronary artery disease. N Engl J Med 2005; 352: 1685-1695.
[43] Lindahl B, Toss H, Siegbahn A, Venge P and Wallentin L. Markers of myocardial damage and inflammation in relation to long-term mortality in unstable coronary artery disease. N Engl J Med 2000; 343: 1139-1147.
[44] Yang Y, Yang L, Liang X and Zhu G. Microrna-155 promotes atherosclerosis inflammation via targeting socs1. Cell Physiol Biochem 2015; 36: 1371-1381.
[45] Thunström E, Glantz H, Fu M, Yucel-Lindberg T, Petzold M, Lindberg K and Peker Y. Increased inflammatory activity in nonobese patients with coronary artery disease and obstructive sleep apnea. Sleep 2015; 38: 463-471.
[46] Volaklis KA, Smilios I, Spassis AT, Zois CE, Douda HT, Halle M and Tokmakidis SP. Acute pro- and anti-inflammatory responses to resistance exercise in patients with coronary artery disease: a pilot study. J Sports Sci Med 2015; 14: 91.

Table S1. Kendall, Spearman and Pearson correlation analyses of the expression of mir-367 with the levels of IL-6, TNF-α and NF-κB in the plasma of CAD patients

			Mir-367	IL-6	TNF-α	NF-κB
Kendall Correlation	Mir-367	Kendall Correlation	1	0.45462*	0.38235*	0.40374*
	Mir-367	Significance	--	2.93E-07	1.62E-05	5.41E-06
	IL-6	Kendall Correlation	0.45462*	1	0.36811*	0.40532*
	IL-6	Significance	2.93E-07	--	3.29E-05	4.94E-06
	TNF-α	Kendall Correlation	0.38235*	0.36811*	1	0.37259*
	TNF-α	Significance	1.62E-05	3.29E-05	--	2.70E-05
	NF-κB	Kendall Correlation	0.40374*	0.40532*	0.37259*	1
	NF-κB	Significance	5.41E-06	4.94E-06	2.70E-05	--
Spearman Correlation	Mir-367	Spearman Correlation	1	0.50788*	0.47416*	0.47452*
	Mir-367	Significance	--	3.44E-05	1.30E-04	1.28E-04
	IL-6	Spearman Correlation	0.50788*	1	0.48474*	0.51973*
	IL-6	Significance	3.44E-05	--	8.68E-05	2.08E-05
	TNF-α	Spearman Correlation	0.47416*	0.48474*	1	0.46321*
	TNF-α	Significance	1.30E-04	8.68E-05	--	1.94E-04
	NF-κB	Spearman Correlation	0.47452*	0.51973*	0.46321*	1
	NF-κB	Significance	1.28E-04	2.08E-05	1.94E-04	--
Pearson Correlation	Mir-367	Pearson Correlation	1	0.42367*	0.34668*	0.59001*
	Mir-367	Significance	--	7.43E-04	0.00666	7.01E-07
	IL-6	Pearson Correlation	0.42367*	1	0.45537*	0.39996*
	IL-6	Significance	7.43E-04	--	2.56E-04	0.00154
	TNF-α	Pearson Correlation	0.34668*	0.45537*	1	0.29667*
	TNF-α	Significance	0.00666	2.56E-04	--	0.02135
	NF-κB	Pearson Correlation	0.59001*	0.39996*	0.29667*	1
	NF-κB	Significance	7.01E-07	0.00154	0.02135	--

*indicates statistically significant correlation among analyzed variables.